Received: 10 November 2024 | Revised: 11 February 2025 | Accepted: 16 March 2025

DOI: 10.1002/aic.18831

AIChE JOURNAL

RESEARCH ARTICLE

Particle Technology and Fluidization

The transition from the fixed to the fluidized state of well-mixed binary-solid mixtures in a liquid upflow

Renzo Di Felice[1] | Filippo Marchelli[1,2]

[1]Department of Civil, Chemical and Environmental Engineering, University of Genova, Genova, Italy

[2]Department of Civil, Environmental and Mechanical Engineering, University of Trento, Trento, Italy

Correspondence
Renzo Di Felice, Department of Civil, Chemical and Environmental Engineering, University of Genova, Genova, Italy.
Email: renzo.difelice@unige.it

Abstract

In this work, an investigation of the transition from fixed to fluidized state of initially homogeneous binary-solid mixtures due to an upward liquid flux was carried out. Like for analogous gas systems, it was confirmed that the full transition occurs over a range of fluid velocities, from the initial to the final fluidization velocity. Based on fluid dynamic equilibrium considerations, we proposed a simple model that quantitatively predicts the different bed configurations as a function of fluid velocity. Thanks to the model, all the mixtures were categorized into four regions, which determined their behavior during the transition process. Extensive experimental investigations supported model predictions, offering insights that had not been reported in previous studies.

KEYWORDS

binary-solid mixture, flotsam and jetsam, fluid-solid forces, minimum fluidization velocity, particle segregation

1 | INTRODUCTION

Basic and applied research on fluidized systems behavior has been carried out for nearly 100 years now, but despite the often-overwhelming scientific production, some basic knowledge gaps are still far from being satisfactorily addressed. This statement is valid for fluidized suspensions made up of a single solid type, but more so when two or more solids are fluidized in the same column, with the fluid dynamic interaction between the fluid and the solids or the solid-solid interaction difficult to put in a quantitative footing. As a result, it is challenging to confidently predict the key features of such a system, for example, bed expansion or the extent of mixing and so on. Recently, Zhang et al.[1] reviewed multi-solid fluidized beds, focusing on their main flow patterns and applications.

This work tackles a specific knowledge gap: understanding how a perfectly mixed binary solid mixture behaves when an upward fluid flux is gradually increased, stepwise, from zero to the point where both solids are fully fluidized. In other words, it examines how the transition from the fixed to the fluidized state takes place. A similar investigation was presented by one of us a few years ago for a similar problem, with the difference that the solids were initially in a completely segregated state.[2] The relevance of the particle-wall interaction was highlighted there as one of the main factors governing the whole process.

The problem is not new by any means as this aspect also has practical implications: an example is the industrial process of classification, where the difference in size and density is exploited to separate different solids.[3] Nonetheless, the present state of the art is quite unsatisfactory: researchers have mostly focused on the behavior of binary mixtures in full fluidization conditions, examining phenomena such as particle segregation and layer inversion, leaving the beginning of fluidization unexplored.

Observations in gas-solid fluidized beds have been more numerous[4–6] possibly due to their higher simplicity of operation and their application in thermochemical processes. However, their behavior is more chaotic, complicating the development of correlations.

Most notably, the research group of Formisani focused extensively on binary gas-solid fluidized beds, covering various aspects of their description.[7–10] In their works, they reported that the transition from the fixed to the fluidized state of a binary-solid mixture takes place over a range of fluid velocities, with the limiting ones named initial (u_{if}) and final fluidization velocities (u_{ff}). While calculating the first is rather straightforward, for the second more problems arise: these authors proposed a model to find its value, but the model is not fully predictive and still relies on experimental observations to estimate some parameters.

Next to the extremely relevant contribution by Formisani et al., a few more gas fluidization articles are related to the purpose of this study. One is the work by Rao et al.,[11] who attempted a classification of the gas fluidization behavior of binary mixtures by relating it to the size and density ratios of the two solids. In this classification, they identified seven different mixture categories, but their work is more concerned with established fluidization conditions, rather than the transition from the fixed to the fluidized state. A very important contribution on incipient gas fluidization was performed by Di Maio et al.,[12] who mainly focused on binary mixtures of large and light particles and small and dense particles. These authors showed that by classifying mixtures according to their diameter and size ratios, three regions can be identified: one where bigger-lighter particles float and fluidize, one where smaller-denser particles tend to sink and fluidize, and one where smaller-denser particles tend to float and fluidize. Their work is, however, only concerned with the onset of the fluidized state and does not discuss the transition from this configuration to the fully fluidized regime. More recently, Liu et al.[13] expanded the latter work by also taking into account other variables, such as the mixture composition and the excess velocity, and by considering the bed voidage more realistically.

Fewer works have investigated this specific aspect dealing with liquid-solid fluidized beds. Asif tried to experimentally determine the minimum fluidization velocity for binary-solid systems[14] by analyzing the pressure drop versus the liquid flow rate, but to do so he considered defluidization runs and his results are therefore not applicable to the present problem. Other works, generally more recently, have also focused on specific aspects, mostly with good results but without providing definitive answers to the overarching questions. For example, Vinnenberg et al.[15] applied the fundamental approach by the group of Formisani for a binary mixture of differently sized glass particles, confirming its general accuracy while commenting on its abovementioned shortcomings.

Other researchers employed instead numerical simulation techniques. Sun et al.[16] tackled the fluidization of an initially mixed binary fixed bed through CFD-DEM simulations: they managed to draw interesting conclusions, showing observations that only numerical simulations can provide, but with the underlying problem that the employed fluid-solid drag model[17] is in principle only valid for stationary spheres, and their use for particles with a non-null relative velocity is an extrapolation. Along this vein, Tiwari et al.,[18] who performed Eulerian-Eulerian simulations of polydisperse liquid fluidized beds, commented that many of the particle-particle force models are also inadequate since they were originally developed for gas-fluidized units. In our more recent study[19] on CFD-DEM simulations of binary mixtures fluidized with water, which only considered same-sized solids, we observed that when starting from perfectly mixed beds the fluid velocity at which the unmixing starts (labeled "critical velocity") always corresponds to the value for which the fluid pressure drop equals the effective bed weight; the two solids become completely unmixed when applying a fluid velocity at least equal to the minimum fluidization velocity of the denser material.

In this framework, the present work tries to shed more light on the transition from the fixed to the fluidized state of binary solid mixtures, using water as the fluidizing agent. We performed an extensive experimental campaign covering a wide range of size and density ratios, and we employed the results to propose a classification and a model to predict how the transition takes place.

2 | MATHEMATICAL DESCRIPTION OF THE PHENOMENON

The system under consideration here is an initially fixed bed of n type solid particles, in the most general case differing in both size and density, homogeneously distributed in the column. Each solid occupies a fraction ε_i of the bed so that

$$\varepsilon = 1 - \sum_{i=1}^{n} \varepsilon_i, \tag{1}$$

is the overall bed voidage. For a mass of solid i charged into the column, M_i,

$$\varepsilon_i = \frac{M_i}{\rho_i V}, \tag{2}$$

with V the overall bed volume (calculated as the product of the column cross-sectional area, A, and the bed height, H), ρ_i the density of solid ith, and the specific solid volume fraction, x_i, is

$$x_i = \frac{\varepsilon_i}{\sum_{1}^{n} \varepsilon_i} = \frac{\varepsilon_i}{1-\varepsilon}. \tag{3}$$

We consider now the case where an upward fluid flow rate is stepwise increased, starting from zero flow. If the interaction between the solids and the column wall is neglected, an overall force balance on the solid phase can quantify the supporting plate distributor reaction, F_{plate}, needed to maintain the solids static (the downwards direction z is taken positive). By introducing the piezometric pressure, P, and with ΔP being its drop across the bed height,

$$F_{\text{plate}} = \sum_{i=1}^{n} \varepsilon_i V[(\rho_i - \rho)g] - A\Delta P, \tag{4}$$

where the term inside the bracket represents the solid effective weight (solid weight minus the classic Archimedes buoyancy).

When the fluid velocity is increased up to a value so that the piezometric pressure equals the effective weight of the solids, the distributor plate reaction will become equal to zero; in other words, the overall fluid-dynamic interaction force is sufficient to support the whole solid bed, allowing the fluidization process to start. For single solid type beds, this point represents the transition from a fixed to a fluidized state (the well-known minimum fluidization velocity, u_{mf}). For multisolid systems, this specific fluid velocity represents the point that can be identified as the velocity of initial fluidization, u_{if}. The estimation of the minimum, or the initial, fluidization velocity can be carried out once the law correlating the pressure drop on the system parameter and fluid velocity is known. For a single solid type with diameter d, this is commonly achieved by using the Ergun equation:

$$\Delta P = H\left[\frac{150(1-\varepsilon)^2\mu}{\varepsilon^3 d^2}u + \frac{1.75(1-\varepsilon)\rho}{\varepsilon^3 d}u^2\right], \tag{5}$$

and numerous correlations based on this approach are available in literature.[20,21]

For multisolid systems, the most common approach to identify u_{if} has been so far based on modifying the Ergun equation by introducing the concept of hydraulic diameter. For spherical particles, it coincides with the Sauter mean diameter:

$$d_h = \frac{1}{\sum \frac{x_i}{d_i}}. \tag{6}$$

This approach has proved to be quite successful in the quantification of the overall bed piezometric pressure drop for binary-solid systems, for which a considerable amount of experimental evidence is available.[22] However, it is not sufficient in completely describing multisolid component beds. In these, a quantification of the forces acting on each solid type is necessary, and the equations cannot predict their values.

At initial fluidization velocity conditions, the force balance for the specific solid type i will be

$$\varepsilon_i V\left[(\rho_i-\rho)g - \frac{6}{\pi d_i^3}f_i^d - \frac{\Delta P}{H}\right] + \sum_{j=1}^{n\,(j\neq i)} F_{ij}^c = 0, \tag{7}$$

where the terms inside the bracket respectively represent the particle effective weight, the drag force on the particle due to the solid-fluid relative velocity and the additional contribution brought about by the pressure gradient. F_{ij}^c is the overall solid-solid contact force exchanged between particle type i and particle type j, with $F_{ij}^c = -F_{ji}^c$. Contrary to ideal monocomponent beds, contact force will always be non-null for multisolid beds even at u_{if}, as the effective particle weight is not balanced by the overall fluid-solid interaction force for each individual solid type.

The relation between piezometric pressure drop and individual drag force on each single particle type is

$$\frac{\Delta P}{H} = \frac{1}{\varepsilon}\sum_{i=1}^{n}\frac{6\varepsilon_i}{\pi d_i^3}f_i^d, \tag{8}$$

and summing all the force balances written for each particle type leads to the overall, well-known, expression

$$\frac{\Delta P}{H} = \sum_{i=1}^{n}\varepsilon_i[(\rho_i-\rho)g]. \tag{9}$$

In the last two decades, the advance of computational techniques has allowed researchers to perform direct numerical simulations of polydisperse particle-fluid systems, which can yield the exact magnitude of the force acting on each particle type. The obtained force magnitudes can be then employed to develop empirical correlations. These are generally expressed as the product of two terms: the average force acting on all particles ($\widehat{f}_i^d$), and a correction factor (β_i) that is specific for each solid type and that depends on its local relative abundance in the mixture. Various correlations are available and a superior one has not yet emerged[22]; however, for our current purposes, we have considered the one proposed by Rong et al. in 2014,[23] which has the advantage of being continuous with the bed composition. Its equations are as follows:

$$\widehat{f}_i^d = \left(0.63 + 4.8Re_i^{-0.5}\right)^2\frac{Re_i}{24}\varepsilon^{-\chi}, \tag{10}$$

$$\chi = 2.65(\varepsilon+1) - (5.3-3.5\varepsilon)\varepsilon^2\exp\left(-\frac{(1.5-log_{10}Re_i)^2}{2}\right), \tag{11}$$

$$\beta_i = \frac{0.5\varepsilon}{\sum_{j=1}^{N}\varepsilon_j/y_j^2} + 0.5(1-\varepsilon)y_i^2 + 0.5y_i, \tag{12}$$

where y_i is the ratio between the particle diameter and the Sauter mean diameter, while Re_i is the particle Reynolds number.

The above correlations allow the determination of the initial fluidization velocity, once the void fraction of the bed is known. It is a well-known aspect that the voidage for solid mixtures in fixed conditions is dependent on the relative amount of the various solids charged in the column, with values well below those typical of single beds. However, the exact value of this parameter is quite difficult to reproduce experimentally given the effect brought about by the way the solids are charged into the column. Exactly defining the bed height is also difficult due to the irregular shape of its upper surface, and even small errors in its estimation may have a large impact on the calculated voidage if H/d is low (as it is here). Therefore, for the time being, a constant value of 0.4 was assumed in all cases, also simplifying numerical calculations.

Moreover, from now on, we restrict the analysis to binary-solid systems, which will be classified by the use of two parameters, the effective density ratio

$$\rho_{\text{eff},r} = \frac{\rho_L - \rho}{\rho_S - \rho}, \tag{13}$$

and the diameter ratio

$$d_r = \frac{d_L}{d_S}, \tag{14}$$

where the subscripts L and S, respectively, identify the large and small solids; for same-size systems, the subscript L relates to the denser solids.

Representative examples of calculated u_{if} values are depicted in Figure 1 for a same density and a same size binary-particle system, as a function of the small/light particle fraction in the mixture. The figure was obtained by fixing to 4 the diameter ratio for one case, and to 0.22 the effective density ratio for the other. For each value of x_S, the corresponding u_{if} was calculated numerically through a MATLAB code as the value that satisfied Equation (9), with the piezometric pressure drop estimated through the Rong model (Equations (10)–(12)).

The difference in the calculated curve shape is noteworthy, with the same size case being very close to a straight line. The above numerical example shows that u_{if} is somewhat positioned between the minimum fluidization velocities of the monocomponent beds ($u_{mf,L}$ and $u_{mf,S}$) and depends on the relative quantity of the single particle type. Needless to say, had the system been of the type where $u_{mf,L} > u_{mf,S}$, then the curve would have been increasing with x_S.

Moreover, and more importantly, the above correlations can indicate for which solid component the term inside the squared bracket in Equation (7) is positive or negative. When positive, the solid at u_{if} will tend to move downwards (i.e., the jetsam component) once the fluidization process starts, whereas, when negative, the solid will tend to move upwards (i.e., the flotsam component). This estimation is graphically reported in Figure 2 in a generalized map, with the different lines reported for selected values of the original solid mixture composition. The curves were obtained through a MATLAB code by fixing the mixture composition and the diameter ratio and varying gradually the density ratio of a generic binary-solid system in ambient water until the pressure drop estimated through Equation (8) and Equations (10)–(12) equaled the overall solid effective weight, Equation (9). This process was repeated for different values of the particle type volume fraction and diameter ratio, yielding the complete curves shown in Figure 2.

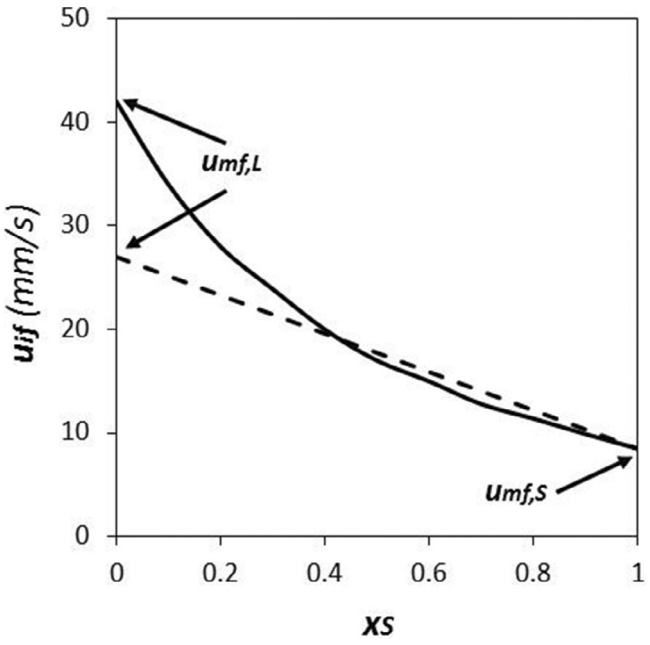

FIGURE 1 Calculated u_{if} for 1 mm glass + 4 mm glass sphere mixture (continuous line) and 1 mm glass + 1 mm iron sphere mixture (dashed line) in ambient water.

In the plot, binary-solid systems positioned above the lines are those where the smaller solid is the flotsam, whereas the opposite will be true for systems positioned below the lines. This result qualitatively resembles the one presented by Di Maio et al.[12] for gas fluidized binary-solid systems. It must also be noted that the addition of fine particles has a dramatic effect for low values of x_S, notably shifting the curve above. The effect is much less marked when they comprise 50% or more of the mixture, or in all cases where the diameter ratio is small.

We move now to describe what happens when the liquid flow rate exceeds u_{if}. An inspection of Equation (7) coupled with the overall pressure drop indicates that contact forces are not capable any longer of keeping the solids stationary, and the solid phases will therefore rearrange their positions until a new configuration is reached.

Given that the initial u_{if} is always in between the two single components u_{mf}, four different scenarios can be expected depending on which of the two solids is the flotsam and if its u_{mf} is larger or smaller than u_{if}.

The above classification can be mapped by using the previous results regarding the flotsam classification and introducing a correlation that quantifies the relative magnitude of the minimum fluidization velocity for the two solid components. Given that Reynolds number at minimum fluidization conditions varies to the power 1 of Archimedes number for viscous suspensions and to the power of 0.5 for inertial suspensions, and considering that the majority of liquid suspensions are in the intermediate regime, we have assumed $Re_{mf} \propto Ar^{0.75}$ which lead to the following correlation describing systems possessing the same minimum fluidization velocity

$$(\rho_L - \rho)^{0.75} d_L^{1.25} = (\rho_S - \rho)^{0.75} d_S^{1.25}. \tag{15}$$

Introducing this result into the generalized maps, three different regions can be individuated, as depicted in Figure 3. Only the curve obtained for x_S equal to 0.5 has been reported as this study focuses on this specific value for the time being.

For type A, the largest particle of the mixture is the floatsam and $u_{mf,L} < u_{if} < u_{mf,S}$; for type B, the largest particles are again the floatsam but $u_{mf,L} > u_{if} > u_{mf,S}$, and for type C, the floatsam component is represented by the smaller particle and again $u_{mf,L} > u_{if} > u_{mf,S}$.

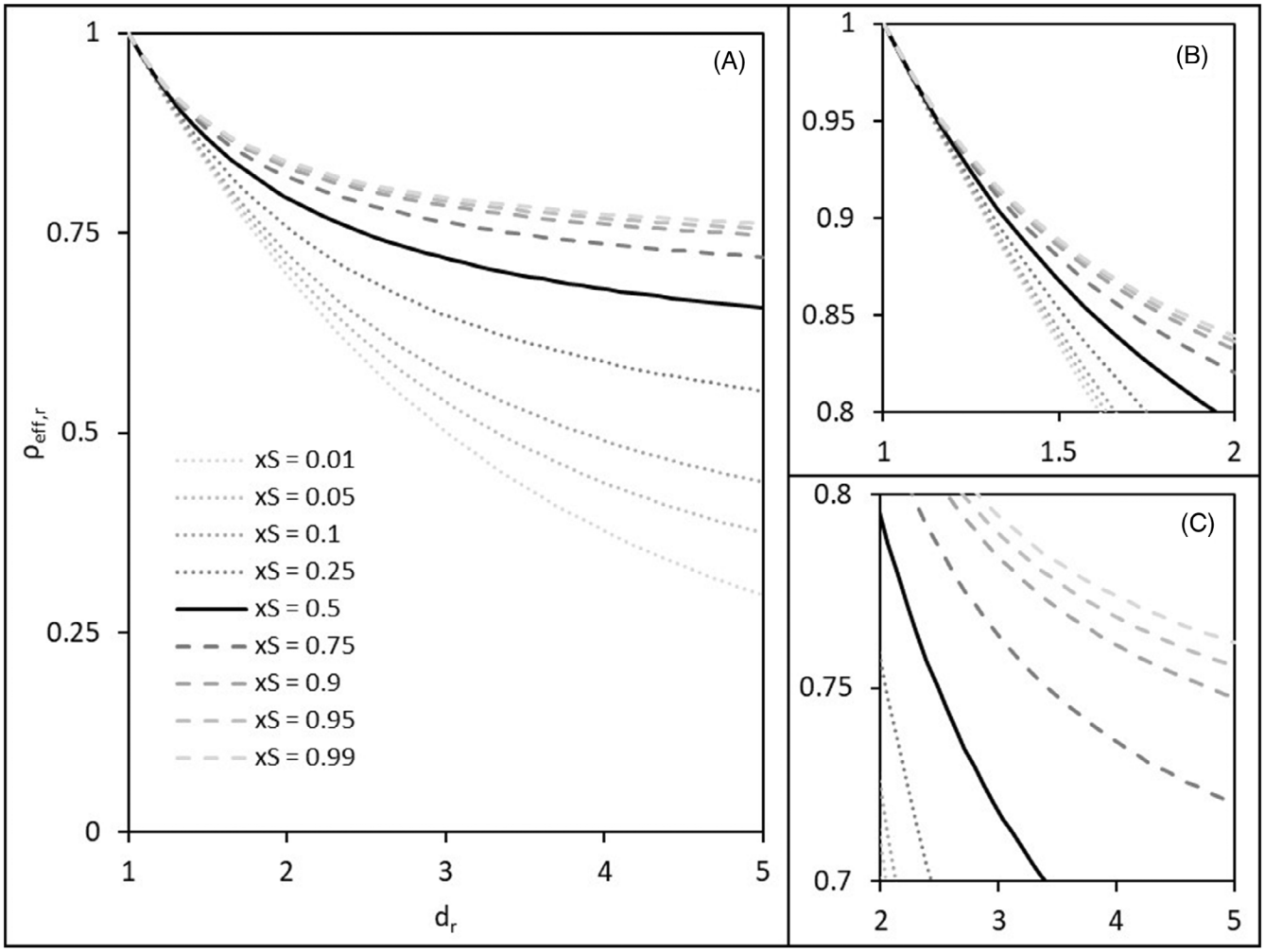

FIGURE 2 General diagram for the identification of the jetsam and flotsam components in a binary-solid mixture suspended by water ((A) is the overall plot, while (B) and (C) are magnifications).

The forth possible combination (smaller particle floatsam and $u_{mf,L} < u_{if} < u_{mf,S}$ has no practical existence) and therefore only three regions are depicted in Figure 3.

The results depicted in Figure 3 are equivalent, and close numerically, to those first reported in Figure 6 by Di Maio et al.,[12] for gas fluidized systems. We have also maintained here their original classification (region A, B, and C).

For the three possible cases depicted in Figure 3, it is understandable that an exact prediction of the arrangement of the particles for velocities larger than u_{if} is impossible to carry out. The reason lies in the difficulty of the numerical quantification of the fluid-solid, solid-solid, and solid-wall interactions. Nevertheless, a limiting, ideal situation can be thought of at least, assuming no restrictions on the particle movement once the velocity exceeds u_{if}. The system may be thought to behave accordingly to the maximum segregation model[24] where the bed was assumed to be made up of two distinct layers: a top, monocomponent one, and a bottom one made up either of one or both solid types, consistently with the overall pressure drop balance. Therefore, we postulate that for a liquid velocity larger than u_{if}, the bed will be composed of two separate layers: a top one made up exclusively of the flotsam component and the bottom one of a composition that satisfies the pressure drop constraint.

With these hypotheses, a description of the transition from the fixed to the fully fluidized state for each single case presented before in Figure 3 can finally be carried out.

2.1 | Type C

The overall process is depicted graphically in Figure 4 for a generic equivolumetric mixture that falls in the type C classification. This kind of mixture is presented first because it is the most straightforward to describe and understand.

The continuous line in Figure 4 represents the calculated values of u_{if} for our specific system. A stepwise increase in the fluid velocity in our process means moving on a vertical line upwards in the figure starting at the center of the x axis. Upon doing so, three different regions are encountered. For $u < u_{if}$, the whole system is in a fixed

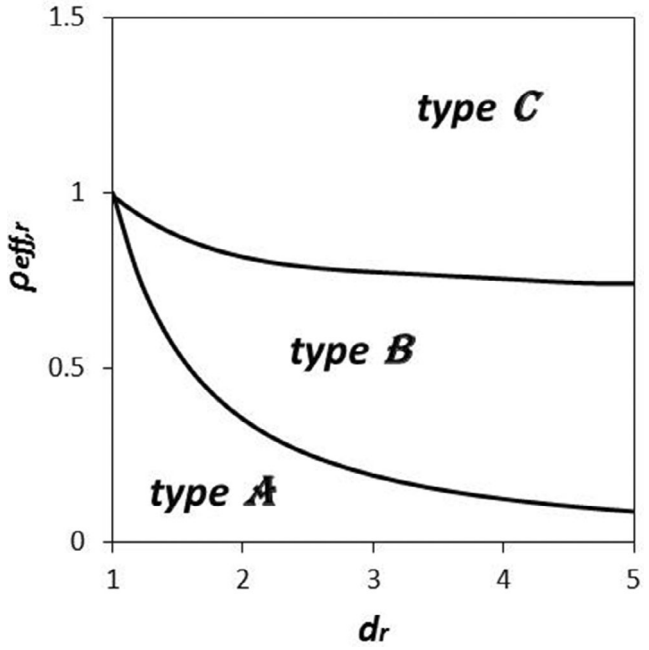

FIGURE 3 General classification of binary-solid mixtures fluidized by water at u_{if}.

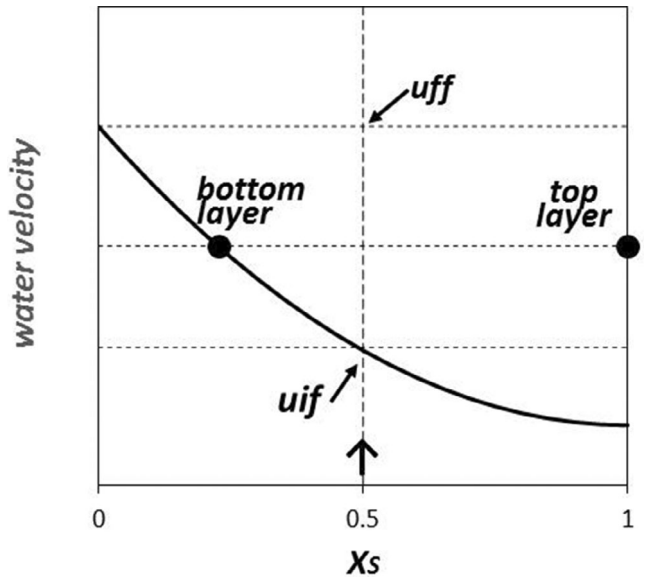

FIGURE 4 Overall depiction of the transition from fixed to fluidized state for a Type C binary-solid mixture.

state, with the overall pressure drop increasing with flow rates. For $u_{if} < u < u_{ff}$, the appearance of a small-component fluidized layer at the top of the bed is expected, with the larger solid and some of the small material forming a bottom fixed layer of particles. The composition of the bottom layer is determined from the x_s-u_{if} curve at that specific velocity where the solids are in equilibrium, whereas an overall mass balance will quantify the relative distribution of the smaller solid in the two layers. It can be seen from Figure 1 that as the smaller particles leave the bottom layer, making it shrink, they remain the floatsam component throughout the whole process. For $u > u_{ff}$, both solids will be fluidized, with u_{ff} coinciding with $u_{mf,L}$. Figure 5 reports the trends of the relative heights of the two layers forming during the transition from the fixed to the fluidized condition. It is also easy to deduce, moreover, that the overall pressure drop will equate to the effective weight of the two solids once u_{if} is reached and will stay at that value for any further velocity increase.

2.2 | Type A

This case is specular to the previous one, and it is represented in Figure 6 for a representative mixture. The monocomponent top layer is made up of the larger solid in a fluidized state, the bottom being a mixture of small and large particles in a fixed state. Inspecting Figure 2 clearly demonstrates that the larger solids remain the floatsam component in this case throughout the whole transition process. A qualitatively similar bed height curve as the one depicted in Figure 5 is predicted, and it is hence omitted for the sake of conciseness. Once again, the overall pressure drop will equate to the effective weight of the two solids for any velocity larger than u_{if}, and u_{ff} will coincide with $u_{mf,S}$.

2.3 | Type B

This is probably the least intuitive situation to describe and is depicted in Figure 7. Once the fluid velocity goes beyond u_{if}, larger solid particles will start to segregate, in a fixed state, at the top of the bed.

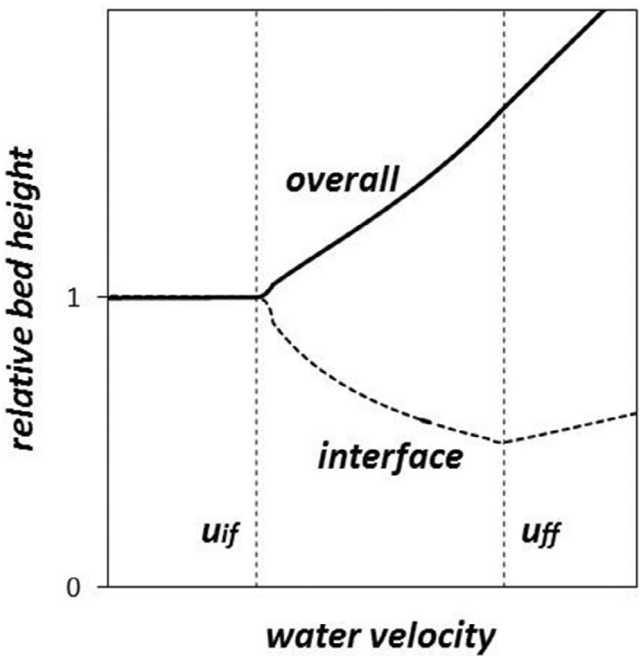

FIGURE 5 Predicted total and bottom layers relative heights for Type C binary-solid systems as a function of water velocity.

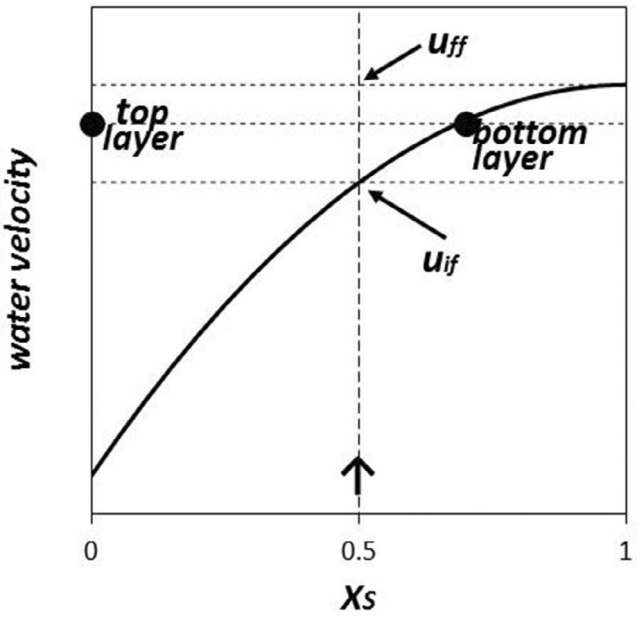

FIGURE 6 Overall depiction of the transition from fixed to fluidized state for a Type A binary-solid mixture.

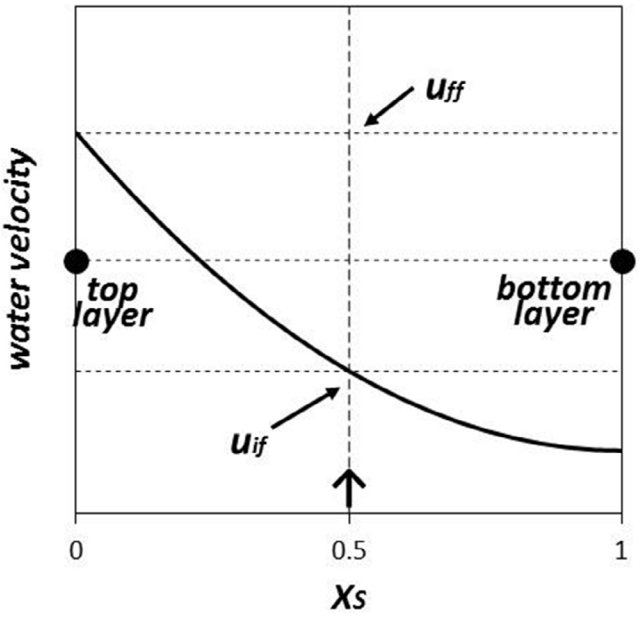

FIGURE 7 Overall depiction of the transition from fixed to fluidized state for a Type B binary-solid mixture.

Contrary to the previous cases, however, the point on the u_{if} curve will not satisfy the overall solid volume balance constraint, and the only remaining option available consistent with the pressure drop constraint is a fluidized layer of smaller particles. As a consequence, the system will consist of a bottom fluidized bed of only smaller particles with a layer of a fixed bed of only larger particles on top, a layer supported by the solid underneath. The separation between the two solids takes place at once, at a velocity just larger than u_{if}, and u_{ff} will

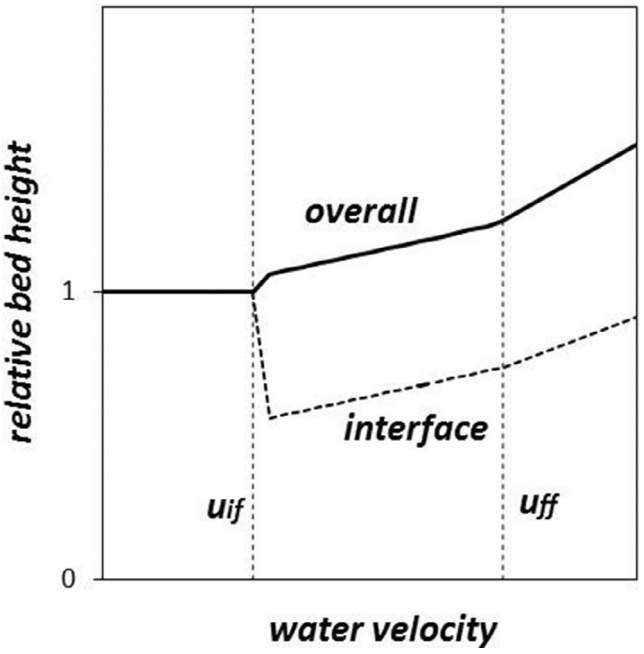

FIGURE 8 Predicted total and bottom layers relative heights for Type B binary-solid systems as a function of water velocity.

be reached for $u = u_{mf,L}$ too. Expected bed and layer heights are depicted in Figure 8, and they are quite different from the previous two cases considered. Again, the overall pressure drop will equate the effective weights of the two solids once u_{if} is reached, even if the top layer is in a fixed state, with the bottom fluidized layer functioning as a distributor and supporting plate.

3 | EXPERIMENTAL SETUP AND PROCEDURE

To confirm the previous considerations, we performed an extensive experimental campaign. The cylindrical column used in this work was made of transparent Perspex, 1500 mm tall and with an internal diameter of 50 mm. It was fed with tap water at ambient conditions, with a fluid density equal to 1000 kg/m^3 and a viscosity very close to 0.001 Pa s (these values were used for all the relevant calculations). Water flow rates were regulated with fine valves, and they were measured with a series of calibrated rotameters. The distributor plate at the bottom of the column was made of sintered brass, and it was followed by a 100 mm layer of lead shots, either 3.4 or 1.7 mm in diameter, which aided the radial homogeneous distribution of the fluid. Whenever an imbalance of the flowing fluid was observed, resulting in internal solid circulation, it led to the dismissal of the experimental run. A pressure probe was positioned just above the layer of lead shots, connected to a pressure transducer with an attached digital display. Pressure readings allowed the quantification of the piezometric pressure drop in the bed for any set flow rate.

Material	Acronym	Density (kg/m^3)	Diameter (mm)	u_{mf} at $\varepsilon = 0.4$ (mm/s)
Zirconia	ZR0.7	3800	0.7	8.5
Lead glass	LG1.0	2850	1.0	10.5
Zirconia	ZR1.2	3800	1.2	19.0
Lead shot	LS1.3	10,800	1.6	60.1
Soda glass	SG1.7	2500	1.7	18.5
Teflon	TF2.0	2100	2.0	18.0
Soda glass	SG2.4	2500	2.4	27.2
Soda glass	SG2.8	2500	2.8	30.5
Acetate	AC4.9	1280	4.8	17.5
Soda glass	SG4.9	2500	4.9	50.5
Delrin	DR14	1450	14	45.8

TABLE 1 Physical parameters and calculated minimum fluidization velocities for the solid utilized in this work.

The solids used were all spherical with a very narrow diameter range. The size was verified with an analog micrometer, considering a representative sample for each solid type. The main solid characteristics (density and size) are reported in Table 1. In the table, the calculated minimum fluidization velocity for ambient water, u_{mf}, is also reported.

The following procedure was adopted for all runs. The desired amount of each material making up the binary mixture was first weighed, to obtain an equivolumetric mixture that, once put in the column, ensured an aspect ratio (H/D) between 1.0 and 1.2. This choice had the objective of minimizing any interactions between the solids and the column wall, such as solid-wall friction or solid bridging (a possibility when larger solids were employed), thus guaranteeing maximum freedom of movement for the particles. Each weighed solid batch was then divided into 10 smaller batches. Two batches of each component were then mixed and dropped into the empty column from the top, with no water inside it. This operation was repeated until the whole mixture was transferred into the fluidizing tube. A quite satisfactory bed of material was obtained in this way with the two solids appearing randomly mixed, and no attempt was made at this stage to modify the arrangement obtained. The initial bed height was estimated visually and recorded, which allowed the overall fixed bed voidage to be evaluated. At this point, the flow rate was increased stepwise starting from zero. For each water velocity, the pressure drop was recorded and the bed visually inspected. The first parameter that was determined was the initial fluidization velocity, u_{if}, which was individuated when the overall bed height had changed and some of the solid had separated and become fluidized. From this point, at each water flow rate, the appearance of the solids was noted, with particular attention to the formation of segregated monocomponent particles in the upper part of the bed, next to the overall height and bottom layer height, when present. The steps were repeated until both solids appeared in a fluidized state, and the resulting final fluidization velocity, u_{ff}, was recorded. A certain degree of subjectivity is obviously inherently present in this determination of u_{if} and u_{ff}, as well as in the evaluation of bed layer heights, but at this stage, this is not considered an important limitation.

4 | SUMMARY OF EXPERIMENTAL OBSERVATION AND COMPARISON WITH PREDICTED BEHAVIOR

An extensive experimental investigation has been carried out to verify how close to reality the description of Section 2 would be. A large number of binary-solid systems were studied, and here only the main and most relevant observations are reported in detail. Specifically, the results are discussed following the previous classification.

4.1 | Type C

The first system reported at length was made up of binary-solid where the larger one was the denser as well: 4.9 mm soda glass spheres mixed with 2 mm Teflon spheres. The difference in minimum fluidization velocity for the two materials is quite large, ensuring a wide range of water flow rates over which the transition from the fixed to the fully fluidized state takes place. Moreover, with the less dense particles being at the same time the smaller, there would be no uncertainty on the fact that it would be the flotsam and segregate at the top of the bed. The overall behavior was indeed much as expected. For water velocity below 25 mm/s, the solids are kept in a fixed state. As the flow rate was increased above this value, a clear layer of the smaller solids could be seen forming at the top of the bed, whereas the larger solids remained in a fixed state at the bottom, together with some of the Teflon particles. Figure 9 visually supports the above description.

The different colors of the solids allow for a clear definition of the layer interfaces, with the top one made up of only Teflon and the bottom of a mixture of Teflon and glass (the darker layer at the very bottom of the picture is the lead utilized to achieve a uniform liquid distribution). This behavior was observed up to a water velocity of

FIGURE 9 Picture of the binary-solid mixture 2.0TF + 4.9SG at a velocity intermediate between u_{if} and u_{ff}.

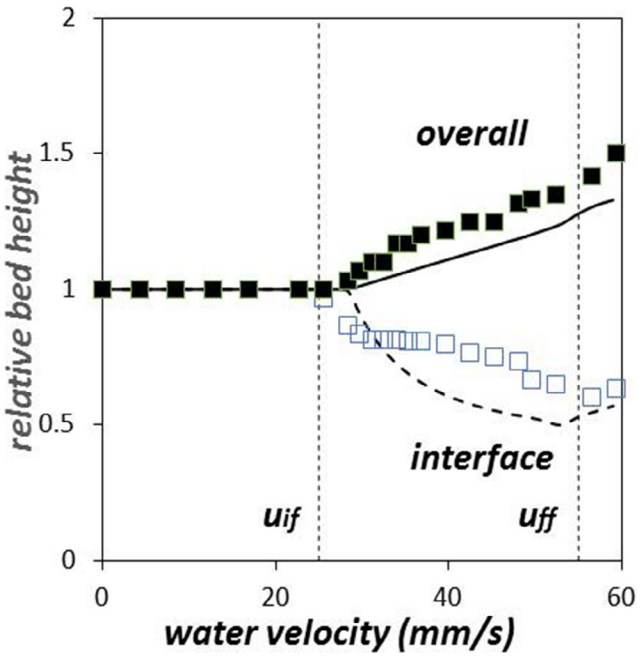

FIGURE 10 Experimental and model layers relative heights as a function of water velocity for the binary system TF2.0 + SG4.9.

55 mm/s, after which both materials could be seen fully fluidized. Observed overall bed heights and interface heights are reported in Figure 10. The Figure also shows the model predictions, qualitatively confirming its correctness. The observed initial and final fluidization velocities, determined as said by visual observation and reported in Figure 10 as vertical lines, are close to the predicted values and the trend of the bed heights, overall as well as the interface, is satisfactorily reproduced.

Measured pressure drop values were as expected increasing when the bed was in a fixed state and then keeping a nearly constant value onward, corresponding to the solid effective weight once the fluidization process had initiated; Figure 11 shows the measured data. The figure shows a quite clear overshoot, after which the pressure drop settles for the expected value (i.e., the solids effective weight). The reason for this overshoot will be briefly discussed in the next section, and the result of ad hoc investigation will be reported in a successive publication. The same qualitative behavior for the pressure drop was observed for all the systems investigated, and it will not be shown again.

The same qualitative behavior was observed for the relevant practical cases of solids differing only in size or in density. Glass particles of 2.4 and 4.9 mm were utilized for the first case, and observed bed heights are depicted in Figure 12, with u_{if} estimated at 34 mm/s and u_{ff} at 59 mm/s. Glass and plastic spheres with a diameter of 4.9 mm made up the same size binary-solid system. In this case, u_{if} and u_{ff} were 37 and 59 mm/s respectively, with bed heights as reported in Figure 13.

Experimental investigations for Type C systems were completed by utilizing two further solid mixtures possessing a density ratio smaller than one, where the solid density and the size act in opposite directions. The main results, together with the previously reported one, are all summarized in Table 2.

4.2 | Type A

The binary-solid systems that fall in this region behave very much as expected: once the u_{if} is reached, the large particles kind forms a

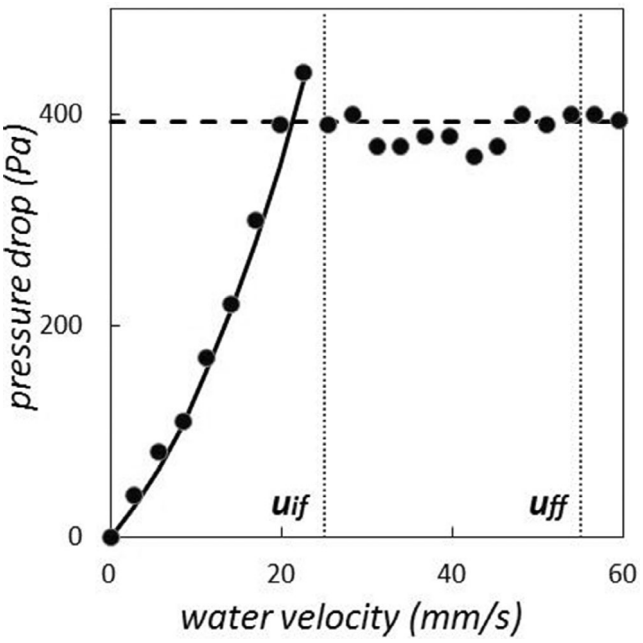

FIGURE 11 Experimental pressure drop for the system TF2.0 + SG4.9 as a function of water velocity. The continuous line is the calculated value for the fixed bed. The horizontal dotted line is the overall effective weight of the solids.

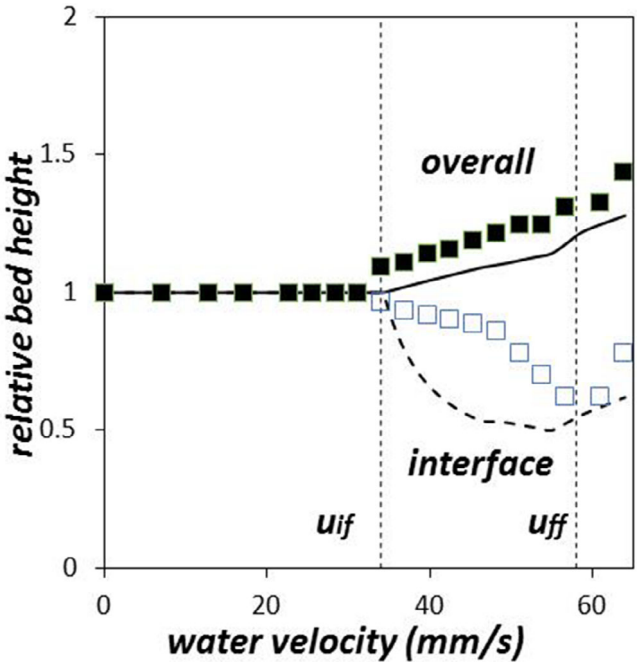

FIGURE 12 Experimental and model layers relative heights as a function of water velocity for the binary system SG2.4 + SG4.9.

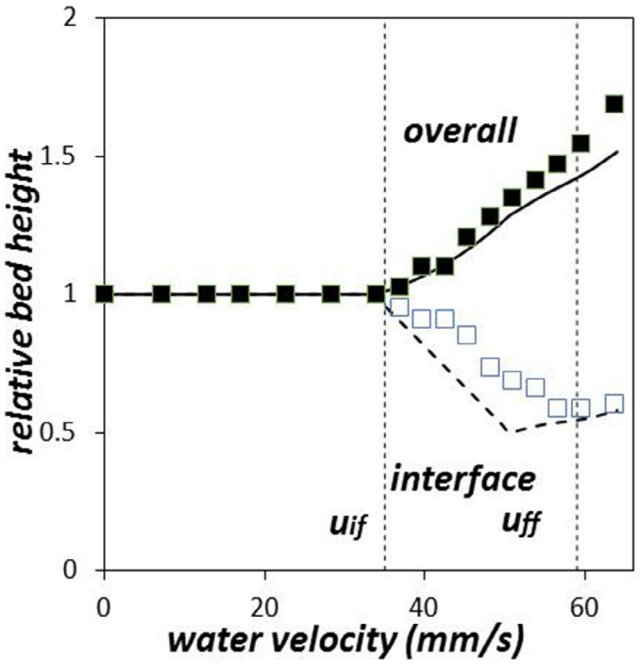

FIGURE 13 Experimental and model layers relative heights as a function of water velocity for the binary system SG4.9 + AC4.9.

fluidized layer above a fixed mixed layer. For the sake of brevity, only one system is reported in detail (2.4 mm glass mixed with 4.9 acetate plastic sphere), with the bed heights as a function of water velocity depicted in Figure 14.

A summary of all the experimental observations for Type A systems is synthesized in the following Table 3.

TABLE 2 Summary of the experimental observations for the Type C binary-solid systems investigated.

System	d_r	$\rho_{eff,r}$	u_{if} (mm/s)	u_{ff} (mm/s)
TF2.0 + SG4.9	2.48	1.36	25	55
SG2.4 + SG4.9	2.06	1.00	34	56
AC4.9 + SG4.9	1.00	5.36	37	59
LG1.0 + SG2.8	2.80	0.81	17	39
LG1.0 + SG4.9	4.85	0.81	17	50

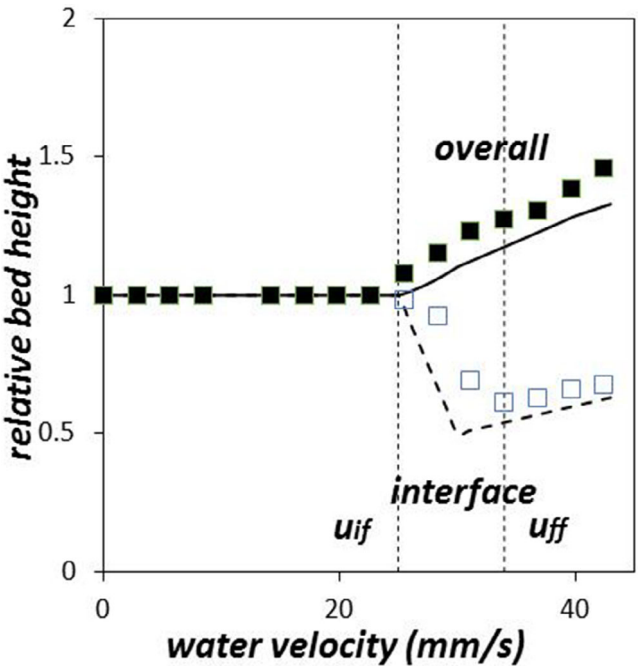

FIGURE 14 Experimental and model layers relative heights as a function of water velocity for the binary system SG2.4 + AC4.9.

TABLE 3 Summary of the experimental observations for the Type A binary-solid systems investigated.

System	d_r	$\rho_{eff,r}$	u_{if} (mm/s)	u_{ff} (mm/s)
LS1.3 + AC4.9	3.67	0.03	36	53
TF2.0 + AC4.9	2.38	0.25	19	25
SG2.4 + AC4.9	2.06	0.19	25	34
SG1.7 + TF2.0	1.18	0.73	20	22

4.3 | Type B

Five of the systems experimentally investigated were located in Region B, and the obtained fluidization velocities are reported in Table 4.

For the Type B region, the expectation once the water flow rate was increased beyond u_{if} was the establishment of a fixed bed layer made up of the larger solids on top of a fluidized layer made up of the smaller solids, with a clear interface separating them. This rather

TABLE 4 Summary of the experimental observations for the Type B binary-solid systems investigated.

System	d_r	$\rho_{eff,r}$	u_{if} (mm/s)	u_{ff} (mm/s)
LG1.0 + AC4.9	4.9	0.15	9	18
SG4.9 + DE14	2.83	0.3	49	55
ZR1.2 + SG2.4	2	0.54	19	33
LG1.0 + SG2.4	2.4	0.78	17	32
ZR1.2 + SG4.9	4.13	0.54	22	46

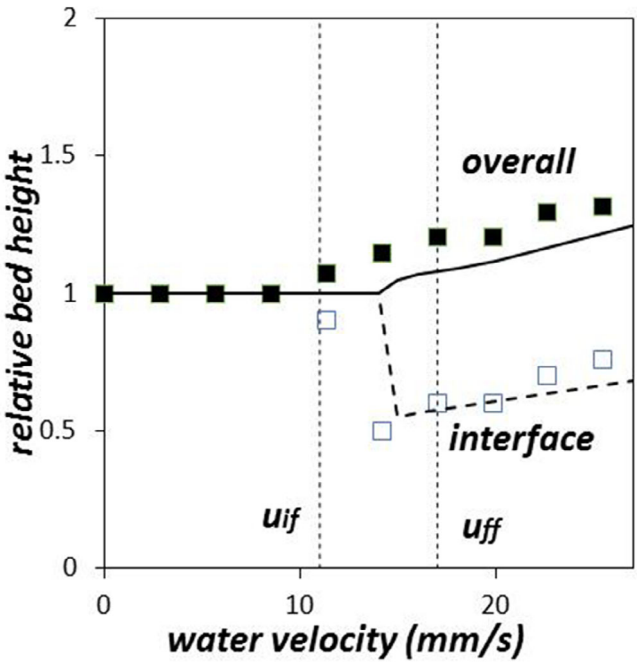

FIGURE 15 Experimental and model layers relative heights function of water velocity for the binary system LG1.0 + AC4.9.

unusual feature was indeed observed for the two top systems in Table 4. Specific results for one of them (LG1.0 + AC4.9) are reported in Figure 15 in terms of layer heights.

The present complete segregation approach, however, completely failed for the three remaining systems in Table 4. For these cases, once the transition to fluidization started, no clear bottom layer interface could be distinguished, and a very strong solid mixing occurred instead. No specific measurements were carried out at this stage of the work to investigate the extent of solid mixing, with visual observation only indicating a stronger presence of the larger solid near the top of the bed.

To produce a first, approximate justification of this discrepancy, we must consider the condition for which a fluidized suspension made up of smaller solids can be able to support an unfluidized bed of larger solids. When the difference between the two solid sizes is considerable, then force analysis can be limited to buoyant contribution.[25] The equilibrium condition will be given by

$$\rho_L = \rho\varepsilon + (1-\varepsilon)\rho_S, \tag{16}$$

which is equivalent to

$$\rho_{eff,r} = (1-\varepsilon), \tag{17}$$

therefore, we expect the fixed bed layer to be supported only for systems possessing a $\rho_{eff,r}$ smaller than the solid volume concentration in the fluidized region.

Consequently, we can tentatively divide region *B* into two subareas, with complete segregation expected for $\rho_{eff,r} < 0.5$, *B*(*I*), and strong solid mixing for $\rho_{eff,r} > 0.5$, *B*(*II*).

5 | SUMMING UP AND DISCUSSION

The present extensive experimental investigation provides strong support for the ideal model suggested earlier, with the transition from the fixed to the fluidized state of binary-solid mixtures taking place over a well-defined range of water velocity, from u_{if} to u_{ff}.

The model presented allows for the estimation of the two boundary velocities as well, with u_{if} calculated through Equation (5) and u_{ff} assumed to coincide with the largest minimum fluidization velocity of the two monocomponent solids. A comparison between estimated and observed values for the velocities is reported in Figures 16 and 17, respectively, with the more than satisfactory agreement evident. It should be remarked here that, as for the monocomponent case, pressure drop measurements are of great help in the quantification of u_{if}, but on the other hand are of no use for the quantification of u_{ff}.

The mild positive deviation between calculated and experimentally observed values for u_{if} can be justified as they were evaluated at a fixed overall bed voidage of 0.4, whereas it is a well-known fact that

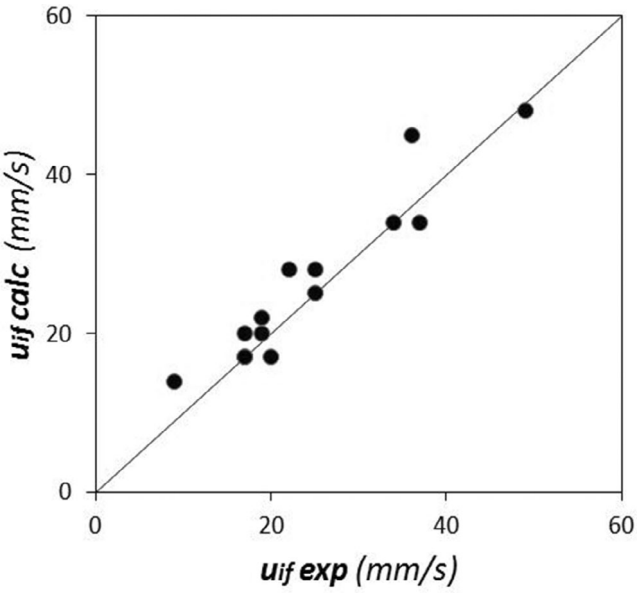

FIGURE 16 Comparison between experimental and calculated u_{if} values.

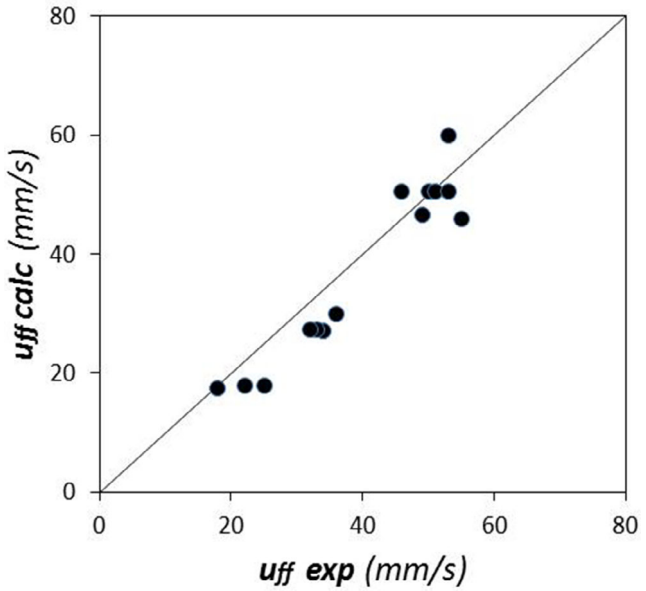

FIGURE 17 Comparison between experimental and calculated u_{ff} values.

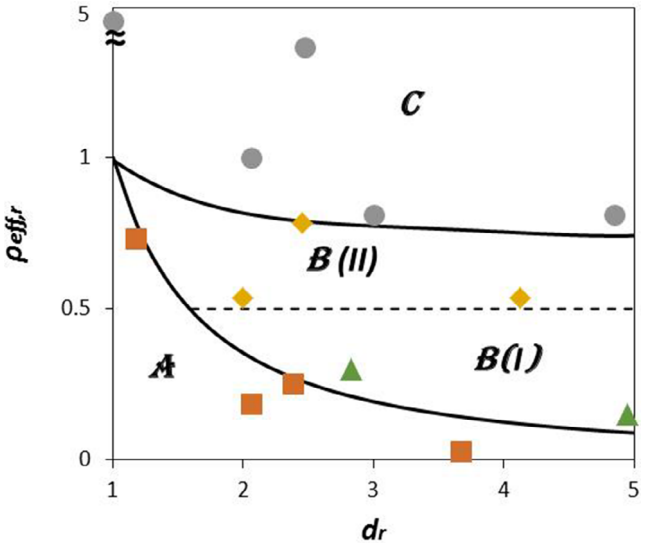

FIGURE 18 Summary of all the systems investigated in this work (circle = Type C; square = Type A; diamond = Type B(I); triangle = Type B(II)) compared with model predictions.

when particles of different diameters are mixed, then the voidage can reach values below those of the corresponding monocomponent bed.

The present approach has proved to represent a good description of the transition process, with the two characteristic parameters of the solids (size ratio and effective density ratio) indicating which solid would segregate at the top of the bed. All the experimental systems investigated in this work are depicted in Figure 18: the encouraging agreement with theoretical predictions is evident. The main open question remains the behavior of the Type B (II) systems, for which further investigation is clearly needed.

It should be stressed here that although the above classification is quite general, it is strictly valid and has been verified for equivolumetric binary-solid mixtures suspended by ambient water. It goes without saying that if the initial solid volume fractions were different, or if the fluid was not ambient water, then the lines separating the different regions would be affected.

The present categorization was able to predict how the interface separating the two solid layers would change with the water flow rate under idealized conditions. A closer examination of the experimental results (Figures 10–15) indicates that the trend is well captured even if the experimental bottom layer heights are generally larger than predictions. This should not come as a surprise: the present model assumes that the solid particles have complete freedom of movement after the fluidization process starts, leading to the formation of a new equilibrium configuration. In reality, however, solid movement is bound to be hindered by solid-solid and solid-wall interactions, and model prediction should be interpreted, therefore, as a limiting, ideal result that real systems may fail to reach.

A further relevant question has to be related to the applicability of the present phenomenological description to systems fluidized by a gas stream. There is no reason why the estimation of u_{if} should not be valid, as only fluid-solid friction governs the process before the transition to the fluidized state takes place. However, once the solid segregation and fluidization on the upper part of the bed come into effect, it is most likely that the whole process will strongly depend on the fluid dynamic behavior of the solid-gas system. Solid-solid interaction and the appearance of gas bubbles will play an important part by promoting solid mixing, with the consequent disruption of the complete segregated idealization. An indirect confirmation of this effect can be seen from the reported experimental observation of Formisani et al.,[7] with u_{ff} differing quite substantially from the largest u_{mf}, as observed here.

Finally, one last aspect has to be mentioned. In all the present experimental observations, pressure drop exhibited an overshoot at u_{if} before leveling off to the expected value corresponding to the overall solid effective weight (see, e.g., Figure 11). This can be justified by considering that, at that velocity, solid-solid interaction force in the vertical direction is not zero, and the occurrence of a solid stress in the vertical direction will automatically result in a solid stress in the radial direction (see Janssenn[26]) with a resulting friction between solid material and column wall. The solid-wall friction force should be considered (even if it was ignored in the present treatment), and a pressure drop larger than the solid effective weight would therefore result. Quantification of this specific aspect is underway.

6 | CONCLUSIONS

In this work, an extensive experimental investigation of the transition from the fixed to the fluidized state of binary-solid homogeneous mixtures has given support to a theoretical model based on

force balance. All the studied mixtures could be characterized in terms of two variables (the diameter ratio and the effective density ratio), which determined their behavior during the transition from the fixed to the fluidized state. Specifically, categories were identified, which differed in terms of which of the two solids tended to move upwards and/or fluidize, with one peculiar case where the two solids tended to mix rather than separate. Moreover, contrary to what was previously reported for gas-solid beds, the initial and final fluidization velocities can be easily estimated analytically, with the latter merely coinciding with the larger of the minimum fluidization velocities of the two solids. The model also allows predicting the height of the two layers during the transition process.

Despite the excellent predicting capability of the theoretical approach, several questions remain unanswered and are currently being investigated. Most notably, we decided not to consider for the time being the influence of the mixture composition on voidage because its experimental estimation is difficult and we believe that it would have brought more uncertainties than advantages. However, this is undoubtedly an aspect worth further investigating.

AUTHOR CONTRIBUTIONS

Renzo Di Felice: Conceptualization; investigation; writing – original draft; writing – review and editing; validation; methodology; data curation; supervision. **Filippo Marchelli:** Conceptualization; investigation; writing – original draft; methodology; validation; writing – review and editing; software; formal analysis; data curation.

ACKNOWLEDGMENT

Open access publishing facilitated by Universita degli Studi di Genova, as part of the Wiley - CRUI-CARE agreement.

CONFLICT OF INTEREST STATEMENT

The authors have no conflicts to disclose.

DATA AVAILABILITY STATEMENT

The raw experimental data reported in this study are summarized in the attached file named "raw experimental data for AIChE journal." Details can be obtained by contacting the author directly. The numerical routine used for obtaining model predictions is available from the authors on demand.

ORCID

Renzo Di Felice https://orcid.org/0000-0002-8169-3325

REFERENCES

1. Zhang L, Fu Z, Li J, Wang R, Bi X. A review on multi-solids fluidized beds. *Powder Technol*. 2023;414:118091. doi:10.1016/j.powtec.2022.118091
2. Di Felice R. Mixing in segregated, binary-solid liquid-fluidized beds. *Chem Eng Sci*. 1993;48(5):881-888. doi:10.1016/0009-2509(93)80327-M
3. Chladek J, Jayarathna CK, Moldestad BME, Tokheim LA. Fluidized bed classification of particles of different size and density. *Chem Eng Sci*. 2018;177:151-162. doi:10.1016/j.ces.2017.11.042
4. Joseph GG, Leboreiro J, Hrenya CM, Stevens AR. Experimental segregation profiles in bubbling gas-fluidized beds. *AIChE J*. 2007;53(11):2804-2813. doi:10.1002/aic.11282
5. Chen JL, Keairns DL. Particle segregation in a fluidized bed. *Can J Chem Eng*. 1975;53(4):395-402. doi:10.1002/cjce.5450530407
6. Olivieri G, Marzocchella A, Salatino P. Segregation of fluidized binary mixtures of granular solids. *AIChE J*. 2004;50(12):3095-3106. doi:10.1002/aic.10340
7. Formisani B, Girimonte R, Longo T. The fluidization process of binary mixtures of solids: development of the approach based on the fluidization velocity interval. *Powder Technol*. 2008;185(2):97-108. doi:10.1016/j.powtec.2007.10.003
8. Formisani B, Girimonte R, Vivacqua V. Fluidization of mixtures of two solids: a unified model of the transition to the fluidized state. *AIChE J*. 2013;59(3):729-735. doi:10.1002/aic.13876
9. Formisani B, Girimonte R, Vivacqua V. The interaction between mixture components in the mechanism of binary fluidization. *Powder Technol*. 2014;266:228-235. doi:10.1016/j.powtec.2014.06.007
10. Girimonte R, Formisani B, Vivacqua V. The relationship between fluidization velocity and segregation in two-component gas fluidized beds: density- or size-segregating mixtures. *Chem Eng J*. 2018;335:63-73. doi:10.1016/j.cej.2017.10.135
11. Rao A, Curtis JS, Hancock BC, Wassgren C. Classifying the fluidization and segregation behavior of binary mixtures using particle size and density ratios. *AIChE J*. 2011;57(6):1446-1458. doi:10.1002/aic.12371
12. Di Maio FP, Di Renzo A, Vivacqua V. A particle segregation model for gas-fluidization of binary mixtures. *Powder Technol*. 2012;226:180-188. doi:10.1016/j.powtec.2012.04.040
13. Liu C, Zhao Y, Li Y, et al. A model for predicting the segregation directions of binary Geldart B particle mixtures in bubbling fluidized beds. *Particuology*. 2024;90:340-349. doi:10.1016/j.partic.2024.01.006
14. Asif M, Ibrahim AA. Minimum fluidization velocity and defluidization behavior of binary-solid liquid-fluidized beds. *Powder Technol*. 2002;126(3):241-254. doi:10.1016/S0032-5910(02)00061-X
15. Vinnenberg S, Ellis N, Bi X, Epstein N. Liquid velocity interval for minimum liquid fluidization of binary solids mixtures. *Can J Chem Eng*. 2017;95(5):985-990. doi:10.1002/cjce.22734
16. Sun H, Yang S, Bao G, Wang H. Particle-scale simulation study of size-induced segregation characteristics of binary particles in a liquid–solid fluidized bed. *Ind Eng Chem Res*. 2023;62(27):10686-10699. doi:10.1021/acs.iecr.3c01493
17. Beetstra R, van der Hoef MA, Kuipers JAM. Drag force of intermediate Reynolds number flow past mono- and bidisperse arrays of spheres. *AIChE J*. 2007;53(2):489-501. doi:10.1002/aic.11065
18. Tiwari SS, Ghatage SV, Joshi JB, Kong B. Segregation and intermixing in polydisperse liquid–solid fluidized beds: a multifluid model validation study. *AIChE J*. 2022;68(8):1-15. doi:10.1002/aic.17725
19. Marchelli F, Di Felice R. A CFD-DEM study of monocomponent and same size binary-solid beds at incipient fluidization. *Powder Technol*. 2022;398:117054. doi:10.1016/J.POWTEC.2021.117054
20. Wen CY, Yu YH. A generalized method for predicting the minimum fluidization velocity. *AIChE J*. 1966;12(3):610-612. doi:10.1002/aic.690120343
21. Grace J, Bi X, Ellis N. *Essentials of Fluidization Technology*. Wiley; 2020. doi:10.1002/9783527699483
22. Marchelli F, Di Felice R. An experimental assessment of fluid–solid drag models based on the pressure drop in bidisperse fixed beds. *Int J Multiph Flow*. 2023;166:104513. doi:10.1016/j.ijmultiphaseflow.2023.104513

23. Rong LW, Dong KJ, Yu AB. Lattice–Boltzmann simulation of fluid flow through packed beds of spheres: effect of particle size distribution. *Chem Eng Sci*. 2014;116:508-523. doi:10.1016/J.CES.2014.05.025
24. Di Felice R. Hydrodynamics of liquid fluidisation. *Chem Eng Sci*. 1995;50(8):1213-1245. doi:10.1016/0009-2509(95)98838-6
25. Di Felice R, Foscolo P, Gibilaro L. The experimental determination of the interaction force on spheres submerged in liquid fluidized beds. *Chem Eng Process Process Intensif*. 1989;25(1):27-34. doi:10.1016/0255-2701(89)85003-2
26. Janssen HA. Versuche über Getreidedruck in Silozellen. *Zeitschr Ver Dtsch Ing*. 1895;39:1045.

SUPPORTING INFORMATION

Additional supporting information can be found online in the Supporting Information section at the end of this article.

How to cite this article: Di Felice R, Marchelli F. The transition from the fixed to the fluidized state of well-mixed binary-solid mixtures in a liquid upflow. *AIChE J*. 2025;e18831. doi:10.1002/aic.18831